

Investigation of hybrid detector structures for surveillance radar with correlated target fluctuations

Nguyen Hoang Nguyen, Pham Viet Anh*, Hoang Minh Thien, Tran Viet Hung

Institute of System Integration, Le Quy Don Technical University, 236 Hoang Quoc Viet, Nghia Do, Hanoi, Vietnam.

*Corresponding author: anhpv.isi@lqdtu.edu.vn

Received 14 Jul. 2025; Revised 23 Sep. 2025; Accepted 10 Oct. 2025; Published 30 Oct. 2025.

DOI: <https://doi.org/10.54939/1859-1043.j.mst.IITE.2025.83-90>

ABSTRACT

This paper investigates the effect of temporally correlated target fluctuations on pulse-train integration efficiency in surveillance radar. A proper complex Gaussian signal model in white noise is assumed. Two hybrid detector structures are synthesized using principal component analysis, where coherent integration is limited to selected subspaces and the remaining components are processed noncoherently. Hybrid-1 restricts coherent integration to the dominant eigen-direction, whereas Hybrid-90 extends it to the subspace capturing 90% of the signal energy. Their performance, measured in terms of detection probability and computational complexity, is evaluated against two widely used reference classes in radar detection: noncoherent energy detection and matched-filter-based coherent integration schemes. The maximum-likelihood detector serves as the optimal benchmark. Monte Carlo simulations across different target fluctuation characteristics and signal-to-noise ratios show that the proposed hybrids achieve a more stable detection probability than conventional schemes while approaching the optimal bound. Hybrid-1, in particular, offers a favorable trade-off between detection reliability and algorithmic complexity. The results provide practical guidelines for surveillance radar design and suggest directions for further research.

Keywords: Surveillance radar; Target detection; Correlated target fluctuations; Coherent integration; Noncoherent integration; Hybrid detector structures.

1. INTRODUCTION

Detection of weak targets in surveillance radar critically depends on the efficiency of signal integration across multiple pulses. Classical approaches fall into two categories: *coherent integration*, typically implemented by matched filtering, and *noncoherent energy detection* [1-5]. Coherent integration achieves near-optimal performance when the target return remains phase-stable over the observation interval, but it is sensitive to temporal fluctuations. *Noncoherent integration* is less efficient but offers robustness under rapid target variations.

Legacy surveillance radars generally employed either fully coherent or fully noncoherent processing, with the operating mode selected according to tactical conditions [1, 3]. Modern systems, however, often extend the integration interval to improve detection sensitivity. In this regime, recent research has emphasized compensation for target motion effects such as Doppler shift, acceleration, and range migration [6-10], whereas the impact of temporally correlated target fluctuations has received comparatively less attention. A limited number of studies have considered combining coherent and noncoherent integration through conventional subaperture processing, where the pulse train is partitioned into temporal segments, coherently integrated within each segment, and then combined noncoherently [11-13]. While effective in mitigating decorrelation over long intervals, this approach relies on a rigid time-domain partition and offers limited adaptability. To address this gap, we investigate *hybrid detector structures* that combine coherent and noncoherent integration in a principled way. The central idea is to exploit dominant signal components through coherent processing while treating residual components noncoherently, thereby balancing detection performance and computational complexity.

Based on the theory of principal component analysis (PCA) [14, 15], two representative hybrid structures are synthesized: Hybrid-1, which performs coherent integration only along the dominant eigen-direction, and Hybrid-90, which extends coherent integration to the subspace capturing 90% of the signal energy, with the remainder processed noncoherently.

The proposed *hybrid structures* are evaluated against two reference classes widely used in radar detection: *noncoherent energy detector* and *matched-filter-based coherent integration schemes*. The *maximum-likelihood detector* serves as the theoretical performance upper bound. Performance is assessed in terms of detection probability and computational complexity through Monte Carlo simulations across different models of target fluctuations and signal-to-noise ratios (SNR). Our main contributions are twofold: (i) a PCA-based synthesis of hybrid detector structures combining coherent and noncoherent integration; and (ii) a performance study against classical detectors, highlighting trade-offs between detection reliability, implementation complexity, and the influence of target correlation in surveillance radar.

The remainder of this paper is organized as follows. Section 2 presents the problem formulation and detector design. Section 3 reports simulation results and discussion. Section 4 concludes.

2. PROBLEM FORMULATION AND DETECTOR DESIGN

2.1. Problem formulation

Let $y \in \mathbb{C}^n$ denote the complex baseband observation vector collected by the radar receiver. Each element of y corresponds to the output of an optimal (or near-optimal) pulse-by-pulse processor, so that n corresponds to the number of pulses collected in a single resolution cell during one antenna scan in surveillance radar. Assuming front-end filtering and interference suppression have been performed, the detection problem can be expressed as a binary hypothesis test:

$$\begin{cases} H_0: y \sim \mathcal{CN}(0, R_0), & \text{(noise only)} \\ H_1: y \sim \mathcal{CN}(0, R_1), & \text{(target + noise)} \end{cases} \quad (1)$$

Under H_0 , the observation consists solely of proper complex Gaussian (PCG) white noise with covariance $R_0 = \sigma^2 I_n$, representing an uncorrelated thermal or clutter background. Under H_1 , the observation includes both noise, $n \sim \mathcal{CN}(0, \sigma^2 I_n)$, and a target return, $s \sim \mathcal{CN}(0, R_s)$, where $R_s \in \mathbb{C}^{n \times n}$ is a Hermitian positive semi-definite covariance matrix characterizing the temporal correlation of target fluctuations across pulses. Assuming independence between signal and noise, the total covariance becomes $R_1 = R_s + \sigma^2 I_n$. This statistical model serves as the foundation for the detector structures developed in the next section.

2.2. Detector design

This section develops and compares six detector structures for the problem formulated in section 2.1. We begin with the optimal maximum likelihood detector, then introduce practical benchmark detectors commonly used in surveillance radar, and finally present the proposed hybrid detectors that combine coherent and noncoherent processing.

2.2.1. Optimal maximum likelihood detector

For $H_0: y \sim \mathcal{CN}(0, R_0)$ and $H_1: y \sim \mathcal{CN}(0, R_1)$, the maximum-likelihood test is [3]:

$$\ln \Lambda(y) = y^H (R_0^{-1} - R_1^{-1}) y - [\text{Indet}(R_1) - \text{Indet}(R_0)] \underset{H_0}{\overset{H_1}{\geq}} 0 \quad (2)$$

Thus, the equivalent quadratic form can be written as

$$T(y) = y^H (R_0^{-1} - R_1^{-1}) y \underset{H_0}{\overset{H_1}{\geq}} \gamma = \text{Indet}(R_1) - \text{Indet}(R_0) \quad (3)$$

For $R_0 = \sigma^2 I_n$ and $R_1 = R_s + \sigma^2 I_n$, consider the eigen-decomposition $R_s = U \Lambda U^H$, where $\Lambda = \text{diag}(\lambda_i, i = 1, \dots, n)$ is diagonal with ordered eigenvalues $\lambda_1 > \lambda_2 > \dots > \lambda_n \geq 0$ and $U = [u_i, i = 1, \dots, n]$ is the corresponding eigenvector matrix [14, 15]. Then

$$R_1 = R_s + \sigma^2 I_n = U (\Lambda + \sigma^2 I_n) U^H; \quad R_1^{-1} = U \text{diag} \left(\frac{1}{\lambda_i + \sigma^2}, i = 1, \dots, n \right) U^H \quad (4)$$

Since $R_0^{-1} = \frac{1}{\sigma^2} I_n$, it follows that

$$R_0^{-1} - R_1^{-1} = U \text{diag} \left(\frac{\lambda_i}{\sigma^2(\lambda_i + \sigma^2)}, i = 1, \dots, n \right) U^H \quad (5)$$

Hence, the test statistic reduces to a weighted sum of projected energies:

$$T(y) = \sum_{i=1}^n \frac{\lambda_i}{\sigma^2(\lambda_i + \sigma^2)} |u_i^H y|^2 \underset{H_0}{\overset{H_1}{\geq}} \gamma = \sum_{i=1}^n \ln \left(1 + \frac{\lambda_i}{\sigma^2} \right) \quad (6)$$

This detector, denoted FullMLD, is optimal under the Gaussian model but requires complete knowledge of the eigenstructure of R_s and becomes computationally intensive for large n .

2.2.2. Classical benchmark detectors

To provide a baseline for evaluating the hybrid approaches, we describe several benchmark detectors commonly adopted in radar systems.

(a) Noncoherent energy detector

Assuming uncorrelated target samples with covariance $R_s = I_n$, the eigenvalues satisfy $\lambda_i = 1, i = 1, \dots, n$, and $V = I_n$. The quadratic form reduces to

$$T(y) = \frac{1}{\sigma^2(\sigma^2 + 1)} \|y\|^2 \underset{H_0}{\overset{H_1}{\geq}} \gamma = n \ln \left(1 + \frac{1}{\sigma^2} \right) \quad (7)$$

This detector, denoted NC-Energy, is the classical noncoherent energy detector. It is computationally simple and robust to target fluctuations but suffers an SNR loss compared with coherent integration.

(b) Fully coherent integration

Assuming perfect correlation across pulses ($\tau = 0$), the covariance reduces to $R_s = \mathbf{1}\mathbf{1}^T$, which is rank-1 with eigenvalue $\alpha_1 = n$ and eigenvector $u_1 = \frac{1}{\sqrt{n}} \mathbf{1}$. The test statistic in (6) becomes

$$T(y) = \frac{1}{\sigma^2(\sigma^2 + n)} |\mathbf{1}^H y|^2 \underset{H_0}{\overset{H_1}{\geq}} \gamma = \ln \left(1 + \frac{n}{\sigma^2} \right) \quad (8)$$

This detector, denoted CMF0, corresponds to a coherent matched filter under the assumption of perfect phase stability.

(c) Matched filter with true correlation

If the target exhibits partial correlation, performance can be improved by aligning with the principal eigenvector of R_s . Assuming R_s is rank-1 with eigenvalue $\lambda_1 = \text{tr}(R_s)$ and decomposition $R_s = \lambda_1 u_1 u_1^H$, the statistic in (6) becomes

$$T(y) = \frac{\lambda_1}{\sigma^2(\sigma^2 + \lambda_1)} |u_1^H y|^2 \underset{H_0}{\overset{H_1}{\geq}} \gamma = \ln \left(1 + \frac{\lambda_1}{\sigma^2} \right) \quad (9)$$

This detector, denoted CMFtrue, adapts to the actual correlation structure but ignores weaker eigenmodes, which may still contain useful signal energy in practice.

2.2.3. Proposed hybrid detectors

The hybrid approach aims to coherently exploit the dominant eigenmodes of the target covariance while processing the remaining energy noncoherently. This synthesis preserves most of the performance benefits of coherent integration while mitigating sensitivity to fluctuations and limiting computational cost. Starting from the general MLT form in (3), each hybrid detector is derived by partitioning the signal covariance matrix R_s and applying selective coherent integration.

The hybrid approach seeks to coherently exploit the dominant eigenmodes of the target covariance while processing the residual energy noncoherently. This design preserves most of the gain from coherent processing while reducing sensitivity to fluctuations and limiting computational cost. Starting from the general maximum-likelihood statistic in (3), each hybrid detector is obtained by partitioning the signal covariance matrix R_s and applying selective coherent integration.

(a) Hybrid-r1

Assume the target covariance is approximated by the dominant rank-1 term plus an isotropic residual:

$$R_s \approx \lambda_1 u_1 u_1^H + \lambda_{\perp}^{(1)} I_n \quad (10)$$

Equivalently, define the residual scalar $\alpha_{\perp} = \frac{\text{tr}(R_s) - \lambda_1}{n-1}$, and approximate

$$R_s \approx \lambda_1 u_1 u_1^H + \lambda_{\perp}^{(1)} (I_n - u_1 u_1^H) \quad (11)$$

Setting $b = \sigma^2 + \lambda_{\perp}^{(1)}$, we obtain

$$R_1 = R_s + \sigma^2 I_n \approx b I_n + \lambda_1 u_1 u_1^H \quad (12)$$

Applying the Sherman–Morrison identity yields

$$R_1^{-1} \approx \frac{1}{b} I_n - \frac{\lambda_1}{b(b + \lambda_1)} u_1 u_1^H \quad (13)$$

Substitution into (3) gives the Hybrid-r1 statistic

$$T(y) = \left(\frac{1}{\sigma^2} - \frac{1}{b} \right) \|y\|^2 + \frac{\lambda_1}{b(b + \lambda_1)} |u_1^H y|^2 = \frac{|u_1^H y|^2}{\sigma^2 + \lambda_1} + \frac{\|y\|^2 - |u_1^H y|^2}{\sigma^2} \underset{H_0}{\underset{H_1}{\geq}} \gamma \quad (14)$$

with threshold $\gamma = \ln(b + \lambda_1) + (n - 1) \ln b - n \ln \sigma^2$.

This isotropic residual approximation trades model fidelity for analytic and implementational simplicity. The resulting test requires only the leading eigenpair and one residual scalar $\lambda_{\perp}^{(1)}$

(b) Hybrid-r90

Let r_{90} denote the smallest integer such that $\sum_{i=1}^{r_{90}} \lambda_i \geq 0.9 \text{tr}(R_s)$. Partition the covariance as

$$R_s \approx U_{r_{90}} \Lambda_{r_{90}} U_{r_{90}}^H + \lambda_{\perp}^{(r_{90})} (I_n - U_{r_{90}} U_{r_{90}}^H) \quad (15)$$

where $U_{r_{90}} = [u_{r_{90}i}, i = 1, \dots, r_{90}]$, $\Lambda_{r_{90}} = \text{diag}(\lambda_i, i = 1, \dots, r_{90})$, and $\lambda_{\perp}^{r_{90}} = \frac{\text{tr}(R_s) - \sum_{i=1}^{r_{90}} \lambda_i}{n - r_{90}}$.

Define $b = \sigma^2 + \lambda_{\perp}^{(r_{90})}$. Then

$$R_1 = R_s + \sigma^2 I_n \approx b I_n + U_{r_{90}} \Lambda_{r_{90}} U_{r_{90}}^H \quad (16)$$

Applying the Woodbury identity for a rank- r_{90} update yields

$$R_1^{-1} \approx \frac{1}{b} I_n - \frac{1}{b^2} U_{r_{90}} \left(\Lambda_{r_{90}}^{-1} + \frac{1}{b} I_{r_{90}} \right)^{-1} U_{r_{90}}^H \quad (17)$$

Thus,

$$R_0^{-1} - R_1^{-1} \approx \left(\frac{1}{\sigma^2} - \frac{1}{b} \right) I_n + \frac{1}{b^2} U_{r_{90}} \left(\Lambda_{r_{90}}^{-1} + \frac{1}{b} I_{r_{90}} \right)^{-1} U_{r_{90}}^H \quad (18)$$

Substitution into (3) gives the Hybrid-r90 test statistic

$$\begin{aligned} T(y) &= \left(\frac{1}{\sigma^2} - \frac{1}{b} \right) \|y\|^2 + (U_{r_{90}}^H y)^H \frac{1}{b^2} \left(\Lambda_{r_{90}}^{-1} + \frac{1}{b} I_{r_{90}} \right)^{-1} (U_{r_{90}}^H y) \\ &= \sum_{i=1}^{r_{90}} \frac{|u_i^H y|^2}{\sigma^2 (\sigma^2 + \lambda_i)} + \frac{\|y\|^2 - \|U_{r_{90}}^H y\|^2}{\sigma^2} \underset{H_0}{\underset{H_1}{\geq}} \gamma \end{aligned} \quad (19)$$

with threshold $\gamma = \ln \det(\Lambda_{r_{90}} + bI_{r_{90}}) + (n - r_{90})\ln b - n\ln\sigma^2$.

This detector requires the r_{90} leading eigenvectors and the residual scalar $\lambda_{\perp}^{(r_{90})}$. It reduces to Hybrid-r1 for $r_{90} = 1$.

3. SIMULATION RESULTS AND DISCUSSION

3.1. Simulation setup and results

To evaluate the six detectors introduced in section 2, two target fluctuation models widely used in the radar literature [1, 3, 5], are considered: $(R_s)_{ij} = \exp(-|i - j|/\tau)$ - The exponential Toeplitz model, which captures correlated Swerling-type fluctuations; and $(R_s)_{ij} = \exp(-(i - j)^2/2\tau^2)$ - The Gaussian model, which represents smoothly decaying correlations.

The simulation parameters are:

- + Signal dimension: $n = 32$.
- + Target fluctuation times: $\tau \in \{0,10,20,100\}$.
- + SNR values: $\{0,10,15,20\}$ dB.
- + Monte Carlo trials: $N_{MC} = 50,000$ per hypothesis.

The following performance metrics are estimated: False alarm probability P_{FA} , miss detection rate probability P_{MS} , and the total error probability $P_{err} = \frac{1}{2}(P_{FA} + P_{MS})$.

Performance is summarized by plots of P_{err} versus SNR for the six detectors: FullMLD, NC-Energy, CMF0, CMFtrue, Hybrid-1, and Hybrid-90. Results are presented separately for the Toeplitz model (figure 1) and the Gaussian model (figure 2).

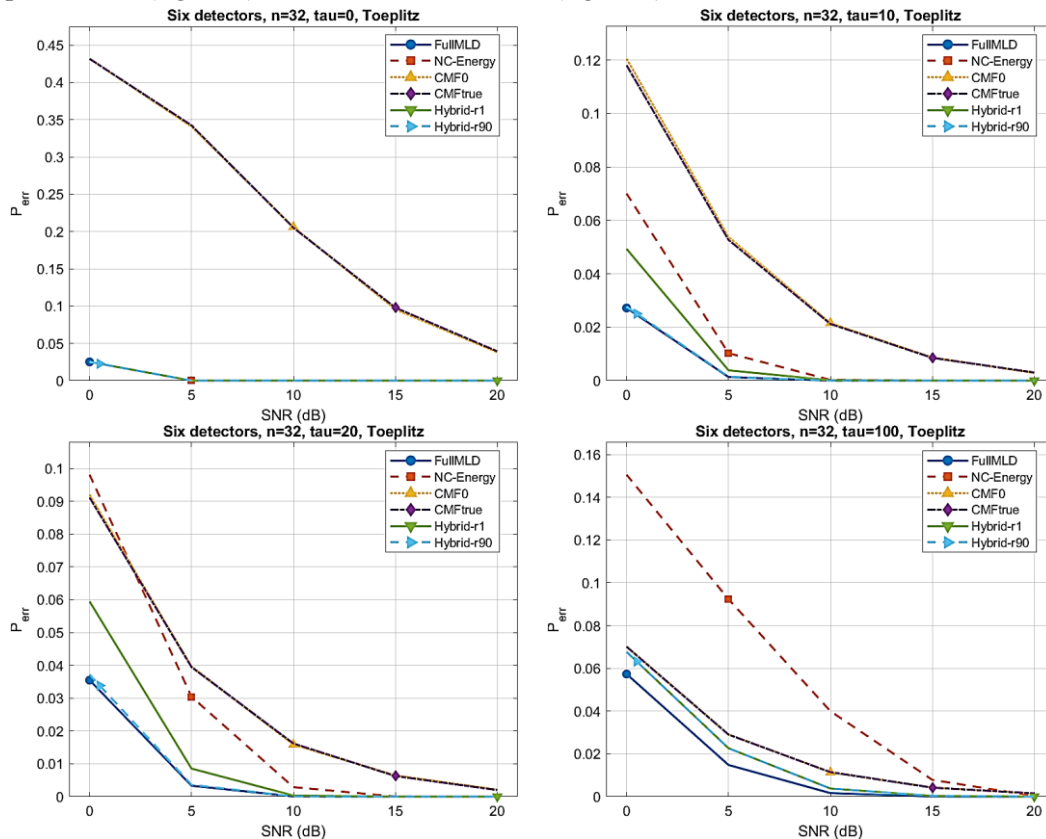


Figure 1. Detection performance under the Toeplitz fluctuation model.

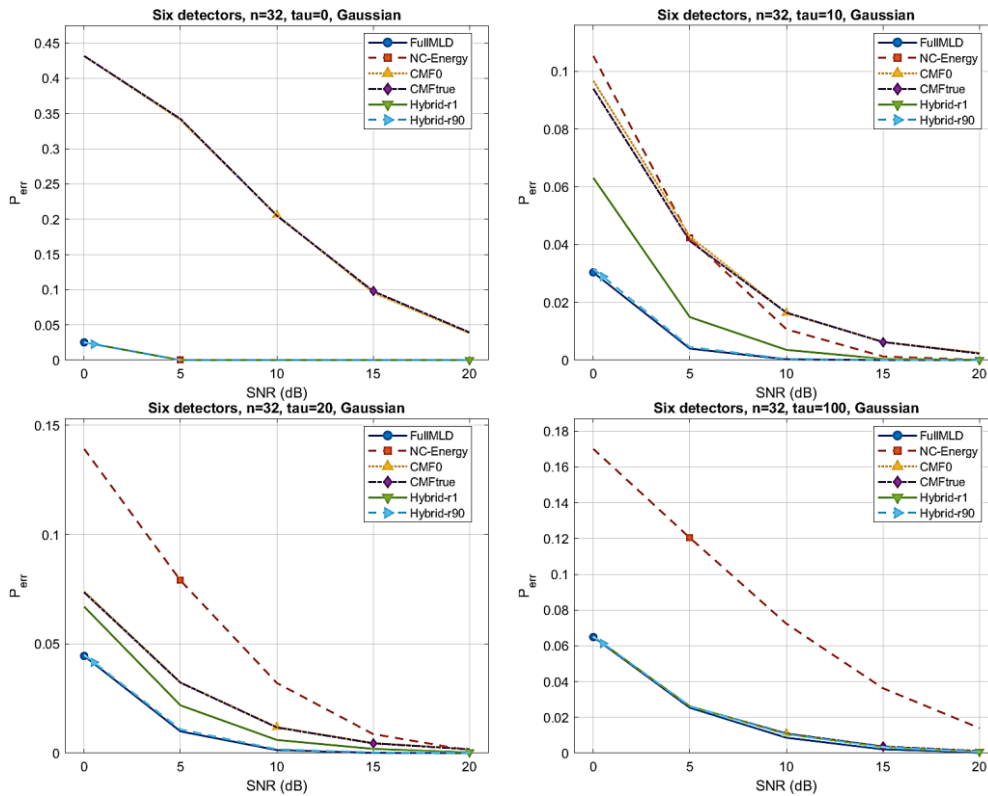


Figure 2. Detection performance under the Gaussian fluctuation model.

3.2. Detection performance evaluation

From figures 1 and 2, several key observations emerge:

General trends: The dependence of error probability P_{err} on SNR follows similar patterns for both Toeplitz and Gaussian fluctuation models. Differences are primarily quantitative, reflecting the distinct τ -dependence of R_S in the two correlation structures.

Coherent integration (CMF0 and CMFtrue): Both detectors yield nearly identical performance since only the dominant signal component is exploited. Coherent integration approaches the FullMLD bound when $\tau \gg n$, but performance degrades rapidly as τ decreases.

Noncoherent integration (NC-Energy): Superior when $\tau \ll n$, as fast decorrelation favors energy accumulation. Performance collapses in highly correlated regimes.

Hybrid detectors (Hybrid-1 and Hybrid-90): These schemes interpolate between coherent and noncoherent extremes. For $\tau \ll n$, Hybrid-1 and Hybrid-90 perform similarly; as τ grows, Hybrid-90 gains an advantage by leveraging a larger coherent subspace. The relative improvement, however, remains modest compared to the gap between pure coherent and noncoherent schemes.

3.3. Complexity considerations and operational recommendations

Complexity Considerations

Two implementation scenarios are distinguished:

Case 1: Precomputed eigen-system (offline)

When eigenvalues and eigenvectors of the covariance matrix are precomputed and stored, all detectors become feasible in real time. The FullMLD requires full matrix–vector multiplications and quadratic forms with complexity $O(n^2)$, which is manageable for moderate dimensions. NC-Energy and CMF0 involve only simple norm or inner product operations of order $O(n)$, while

CMFtrue reduces to a single projection onto the dominant eigenvector, also $O(n)$. The hybrid schemes require additional residual energy computations, yielding complexity $O(n)$ for Hybrid-1 and $O(r_{90}n)$ for Hybrid-90, where $r_{90} \ll n$. Thus, assuming eigen-basis storage, all detectors, including hybrid structures, are real-time implementable.

Case 2: Online eigen-decomposition

If eigenvalues and eigenvectors must be computed in real time, the computational burden rises sharply. FullMLD demands eigen-decomposition of an $n \times n$ Toeplitz matrix $O(n^3)$, which is prohibitive for moderate n . Fast Toeplitz eigensolvers $O(n \log n)$ can mitigate but not eliminate the challenge. NC-Energy and CMF0 remain unaffected and retain $O(n)$ complexity, making them the most practical. CMFtrue and Hybrid detectors depend on extracting the dominant eigenvector; power-iteration methods reduce the cost to $O(kn^2)$, yet remain heavy for real-time applications. Hybrid-90 is particularly demanding as multiple eigenvectors are required.

Operational Recommendation

In practice, NC-Energy and CMF0 offer guaranteed real-time feasibility without precomputation. Hybrid detectors and CMFtrue are viable only when eigenvectors are available from offline computation or dedicated hardware acceleration (e.g., FPGA/ASIC).

With precomputed eigenstructures, all schemes are practically deployable. Among them, Hybrid-r1 achieves the most favorable balance between detection reliability and computational complexity, making it particularly well-suited for operational scenarios. Hybrid-r90 can provide further performance gains in strongly correlated regimes but incurs a higher implementation cost. These observations indicate that hybrid detectors represent a promising middle ground between theoretical optimality and practical feasibility.

4. CONCLUSIONS

This work analyzed the effect of temporally correlated target fluctuations on detection in surveillance radar. Two PCA-based hybrid detectors were synthesized, alongside four reformulated benchmark schemes, yielding a unified set of six representative detectors evaluated via Monte Carlo simulation.

The results clarify the trade-off between coherent and noncoherent processing: coherent methods excel in slow fluctuations but degrade under fast decorrelation, while noncoherent accumulation remains robust but less sensitive. Hybrid schemes alleviate these drawbacks by coherently processing dominant subspaces and treating residual energy noncoherently.

By embedding both classical and hybrid detectors into a common eigenstructure framework, the study exposes their structural relationships and guides implementation choices. The findings demonstrate that hybrids provide a principled compromise between theoretical optimality and practical feasibility. Future research will address robustness under model mismatch and explore hardware-efficient architectures for real-time deployment.

REFERENCES

- [1]. Skolnik, M. *“Radar handbook,”* 3rd ed., New York: McGraw-Hill, (2008).
- [2]. Richards, M. A., Scheer, J. A., and Holm, W. A. *“Principles of modern radar: Basic principles,”* Raleigh, NC, USA: SciTech Publishing, Inc., (2010).
- [3]. De Maio, A., and Greco, M. *“Modern radar detection theory,”* Pisa: University of Pisa, (2016).
- [4]. Weinberg, G. *“Radar detection theory of sliding window processes,”* CRC Press, (2017).
- [5]. De Maio, D., Farina, A., and Foglia, G. *“Target fluctuation models and their application to radar performance prediction,”* IEE proceedings – radar, sonar and navigation, 151(5), 261–269, (2004).
- [6]. Zhang, L., Chen, H., Qu, Q., and Wang, Y. *“Radar non-coherent integration detection for high-speed multiple targets via Doppler frequency compression,”* IEEE transactions on aerospace and electronic systems, 61(2), 3092–3105, (2024).

- [7]. He, Z., Chen, X., Zhang, H., and Zhang, L. “Long-time integration for drone targets detection based on digital ubiquitous radar,” in IEEE 5th international conference on electronic information and communication technology (ICEICT), Hefei, China, 21–23 August 2022, (2022).
- [8]. Zhao, L., Tao, H., Chen, W., and Song, D. “Maneuvering target detection based on subaperture joint coherent integration,” remote sensing, 13(10), 1948, (2021).
- [9]. Liu, G., Tian, Y., Wen, B., and Liu, C. “Combined coherent and non-coherent long-time integration method for high-speed target detection using high-frequency radar,” remote sensing, 16(12), 2139, (2024).
- [10]. Xu, J., Zhou, X., Qian, L., Xia, X., and Long, T. “Hybrid integration for highly maneuvering radar target detection based on generalized radon-fourier transform,” IEEE transactions on aerospace and electronic systems, 52(5), 2554–2561, (2016).
- [11]. Zhou, X., Qian, L., Ding, Z., Xu, J., Liu, W., and You, P. “Radar detection of moderately fluctuating target based on optimal hybrid integration detector,” IEEE transactions on aerospace and electronic systems, 55(5), 2408–2425, (2019).
- [12]. Zhang, Z., Liu, N., Hou, Y., Zhang, S., and Zhang, L. “A coherent integration segment searching based GRT–GRFT hybrid integration method for arbitrary fluctuating target,” remote sensing, 14(11), 2695, (2022).
- [13]. Zheng, H., Zhang, Q., Zhang, Y., and Yan, S. “Hybrid integration detection of moving target with moderately fluctuating RCS,” IET international radar conference (IRC 2023), 47, 4060–4064, (2024).
- [14]. Jolliffe, I. T. “Principal component analysis,” New York: Springer, (2002).
- [15]. Abdi, H., and Williams, L. J. “Principal component analysis,” wiley interdisciplinary reviews: computational statistics, 2(4), 433–459, (2010).

TÓM TẮT

Nghiên cứu cấu trúc bộ phát hiện lai cho ra đa cảnh giới trong điều kiện mục tiêu có thăng giáng tương quan

Bài báo nghiên cứu ảnh hưởng của tính thăng giáng của mục tiêu đến hiệu quả tích lũy chùm xung trong ra đa cảnh giới. Mô hình tín hiệu được giả thiết là proper Gaussian phức trên nền tạp trắng. Hai cấu trúc bộ phát hiện lai được xây dựng dựa trên lý thuyết phân tích các thành phần chính, trong đó một vùng tín hiệu được tích lũy tương quan và xử lý không tương quan cho vùng còn lại. Hybrid-1 chỉ thực hiện tích lũy tương quan theo hướng riêng trội nhất, trong khi Hybrid-90 mở rộng đến không gian con bao hàm 90% năng lượng tín hiệu. Hiệu năng của các cấu trúc này, đặc trưng bởi xác suất phát hiện và độ phức tạp tính toán, được so sánh với hai phương án xử lý thông dụng là tích lũy tương quan và tích lũy không tương quan triển khai dưới dạng bộ lọc phối hợp. Đồng thời chúng được tham chiếu với thuật toán phát hiện tối ưu theo tiêu chuẩn hợp lý cực đại. Các mô phỏng Monte Carlo trong điều kiện thăng giáng nhanh chậm khác nhau cho thấy hai cấu trúc lai đề xuất đạt xác suất phát hiện ổn định hơn so với các sơ đồ thông thường, đồng thời tiến gần đến ngưỡng tối ưu. Riêng Hybrid-1 cho sự cân bằng hợp lý giữa độ tin cậy phát hiện và độ phức tạp tính toán. Những kết quả này cung cấp gợi ý thực tiễn cho việc cải tiến thiết kế ra đa cảnh giới và gợi mở các hướng nghiên cứu tiếp theo.

Từ khóa: Ra đa cảnh giới; Phát hiện mục tiêu; Thăng giáng mục tiêu tương quan; Tích lũy tương quan; Tích lũy không tương quan; Cấu trúc bộ phát hiện lai.